Synergistic Enhancement of Luminescence and Ferroelectricity Driven by (Z)-Clipping of a Tetraphenylethene

Authors: Sewon Lim[+], Donghwan Kim[+], Hee jung Kim, Hwandong Jang, Sienoh Park, and Eunkyoung Kim*

Affiliation:

Department of Chemical and Biomolecular Engineering, Yonsei University, 50 Yonsei-ro, Seodaemun-gu, Seoul, 03722, South Korea

Index of supporting information

S-1. Synthesis and characterization

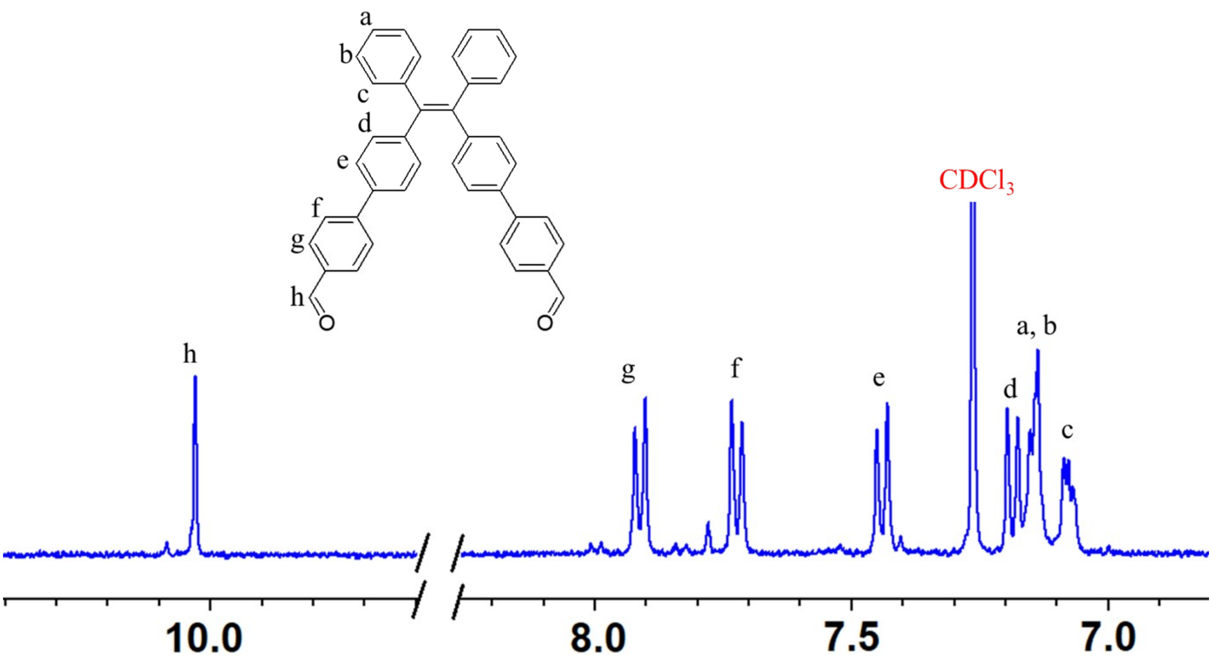

Figure S1. (a) ^{1}H NMR spectrum of TPE2PhCHO-(Z) and comparison with previously reported result.

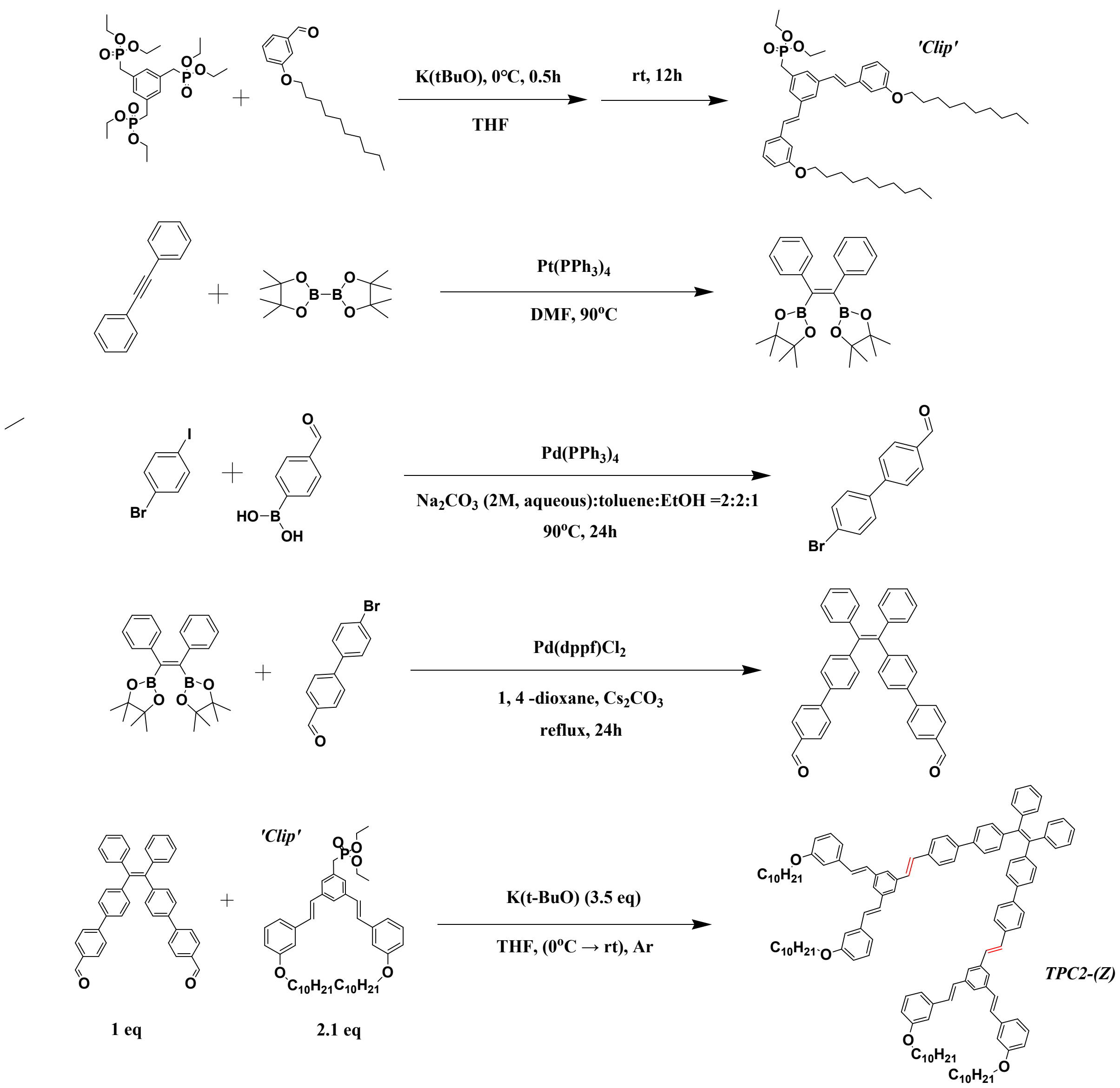

Figure S2. Synthesis schemes of Clip and TPC2-(Z)

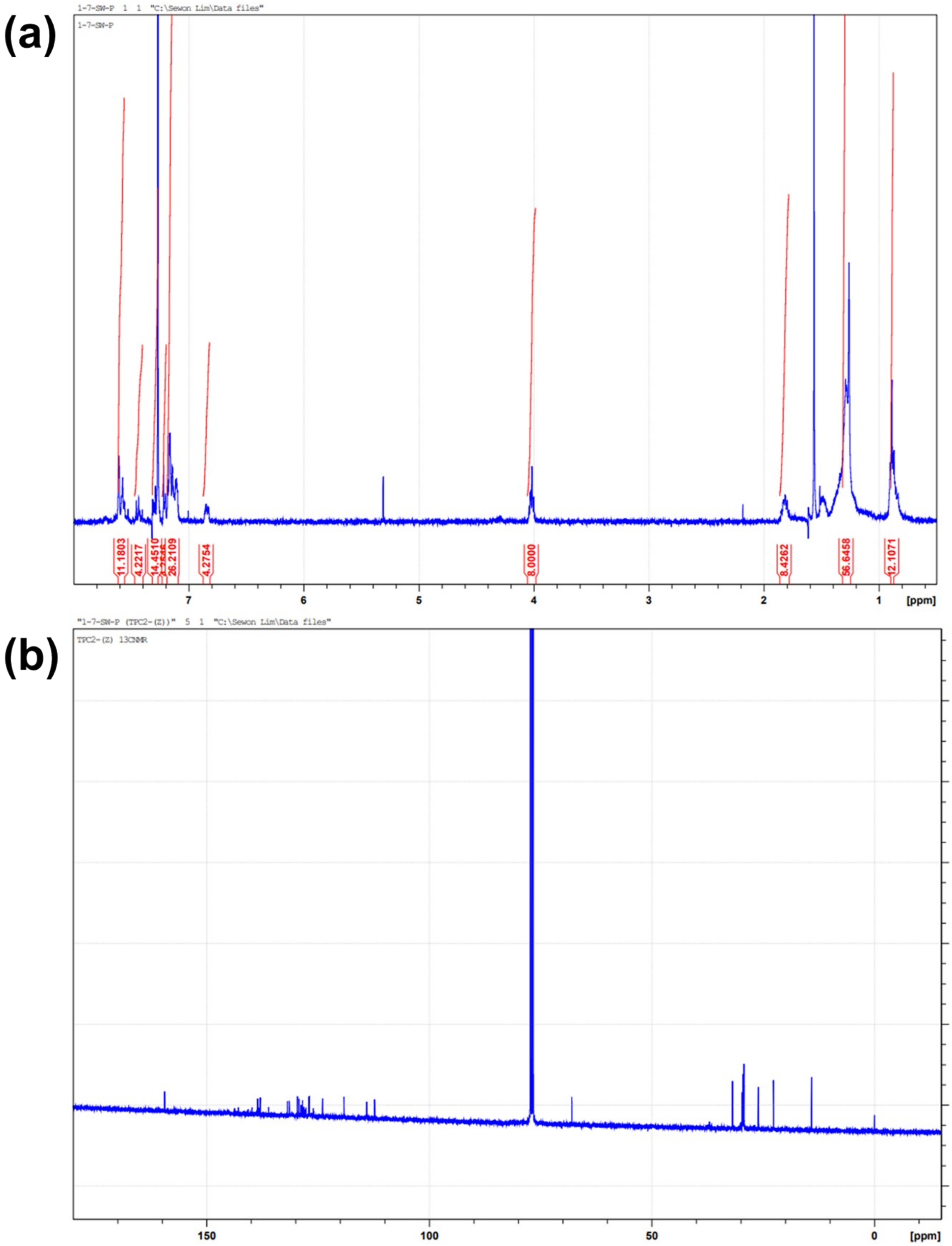

Figure S3. (a) ^{1}H NMR and (b) ^{13}C NMR spectra of TPC2-(Z) on 400 MHz NMR spectrometer

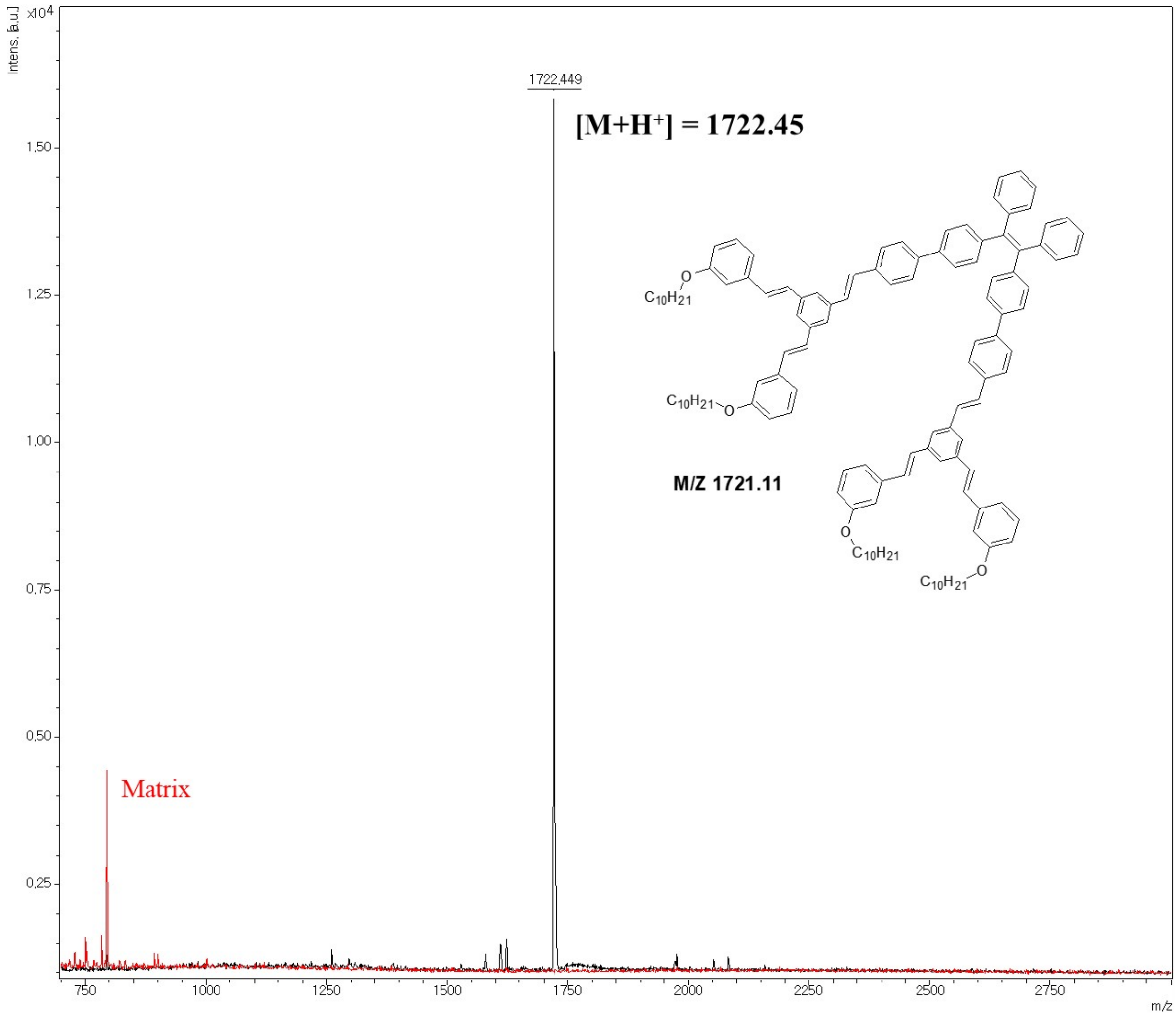

Figure S4. Matrix-assisted laser desorption ionization time-of-flight (MALDI-TOF/TOF) mass spectra of TPC2-(Z)

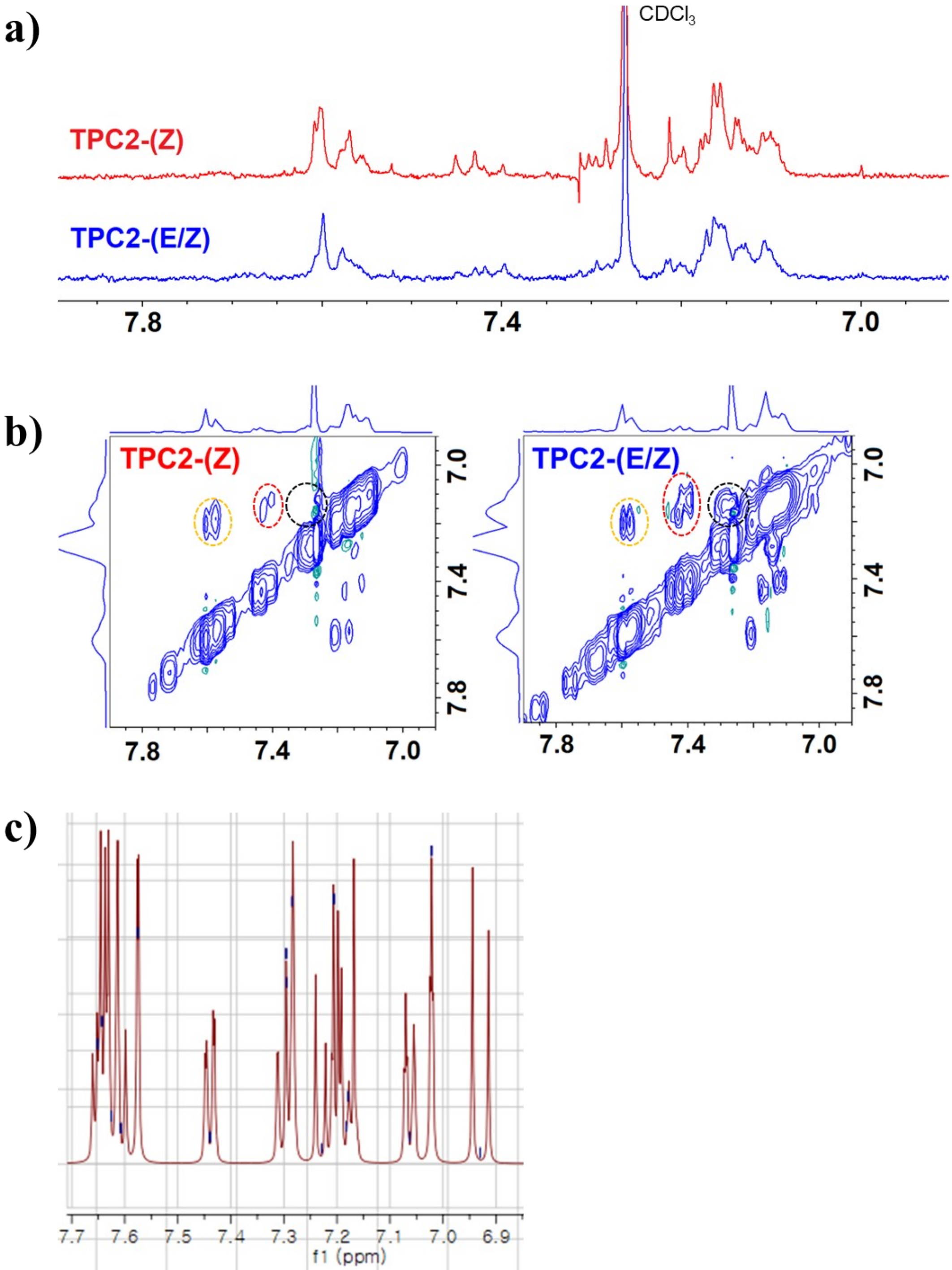

Figure S5. a) [1]H NMR Comparison of TPC2-(Z) and TPC2-(E/Z). b) 2D-NOESY [1]H NMR of TPC2-(Z) and TPC2-(E/Z) between 6.9~7.9 ppm on 400 MHz NMR spectrometer. c) MestReNova [1]H NMR prediction simulation of TPC2-(Z).

S-2. Thermal and electrochemical properties of TPC2-(Z)

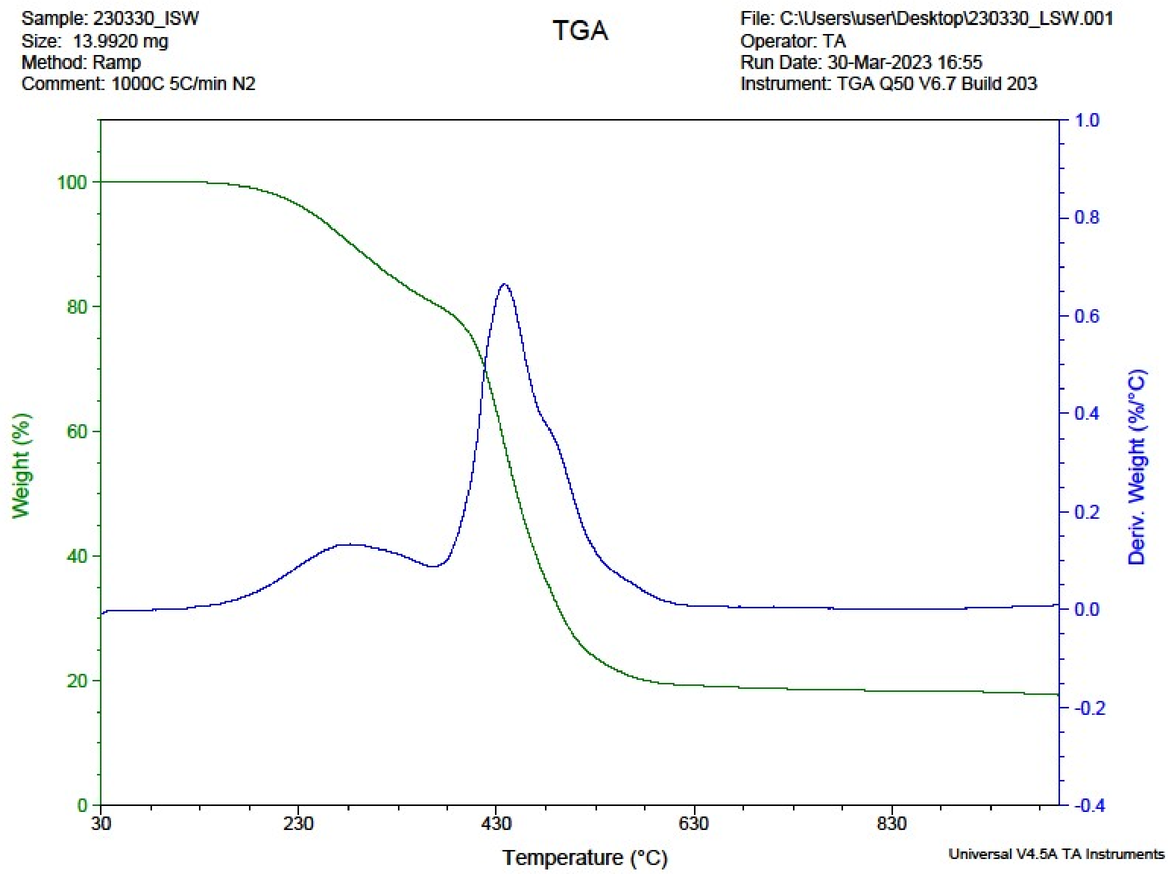

Figure S6. Thermalgravimetric analysis (TGA) measurements of TPC2-(Z)

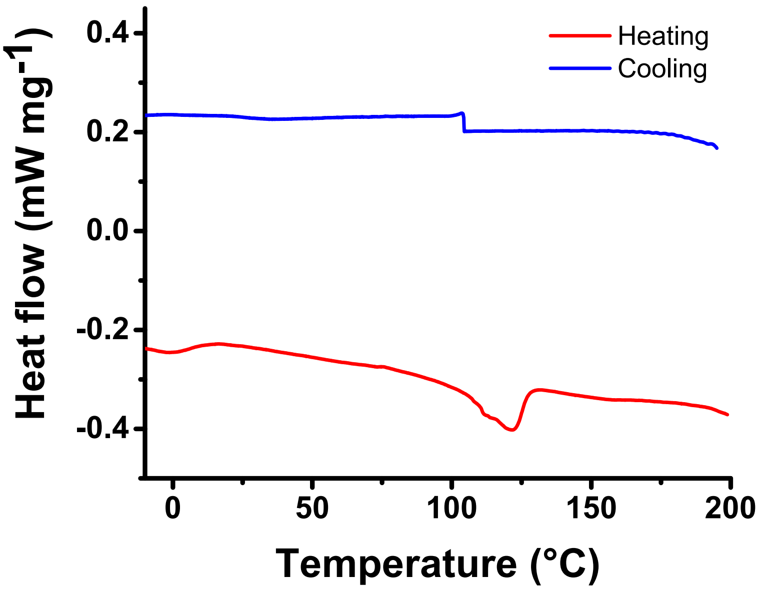

Figure S7. Differential scanning calorimetry (DSC) measurements of the crystalline powder under nitrogen at 10K min^{-1} of TPC2-(Z).

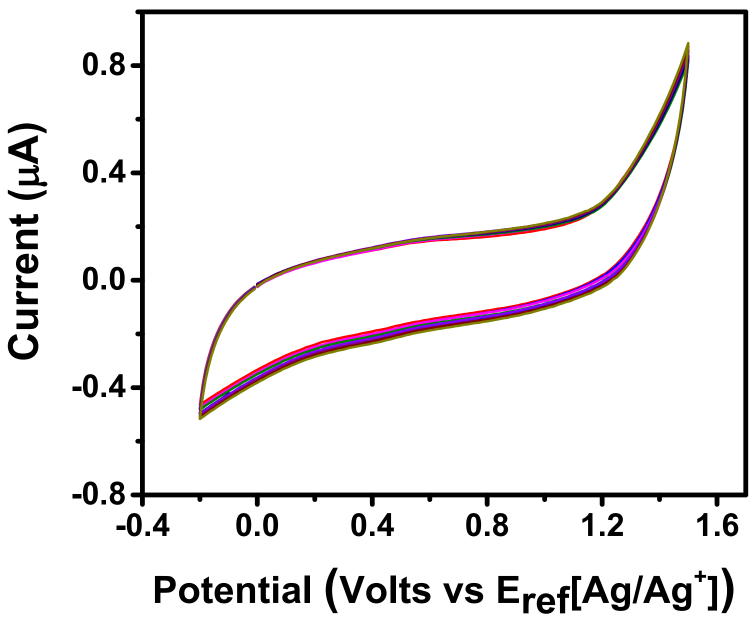

Figure S8. Cyclic voltammograms (CV) of TPC2-(Z) in chloroform with 0.1 M tetrabutylammonium hexafluorophosphate as electrolyte, a platinum disk as working electrode, a platinum wire as counter electrode and an Ag/AgCl reference electrode. The scan rate was 100 mV/s.

S-3. Optical and structural characterization of TPC2-(Z)

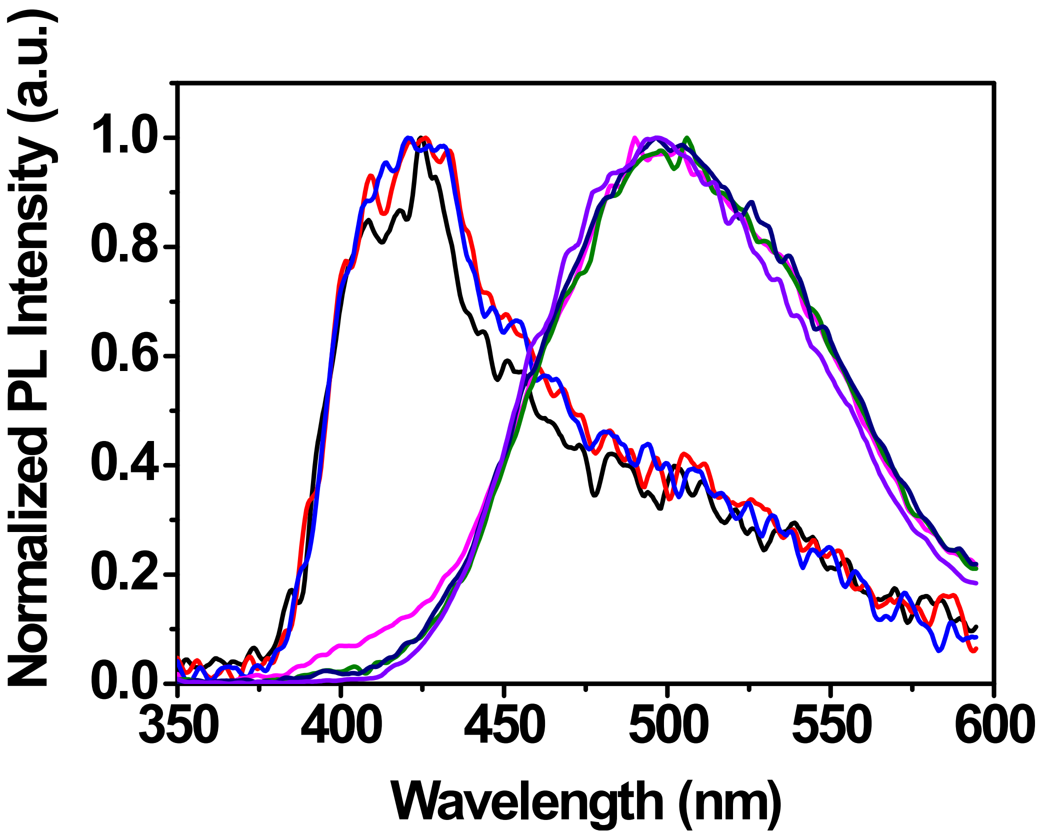

Figure S9. Normalized PL spectra of TPC2-(Z) with different water fractions (0% (black dotted), 10% (red), 30% (blue), 50% (magenta), 70% (green), 80% (navy), 90% (purple) at excitation wavelength 330 nm; at concentration 10^{-5} M).

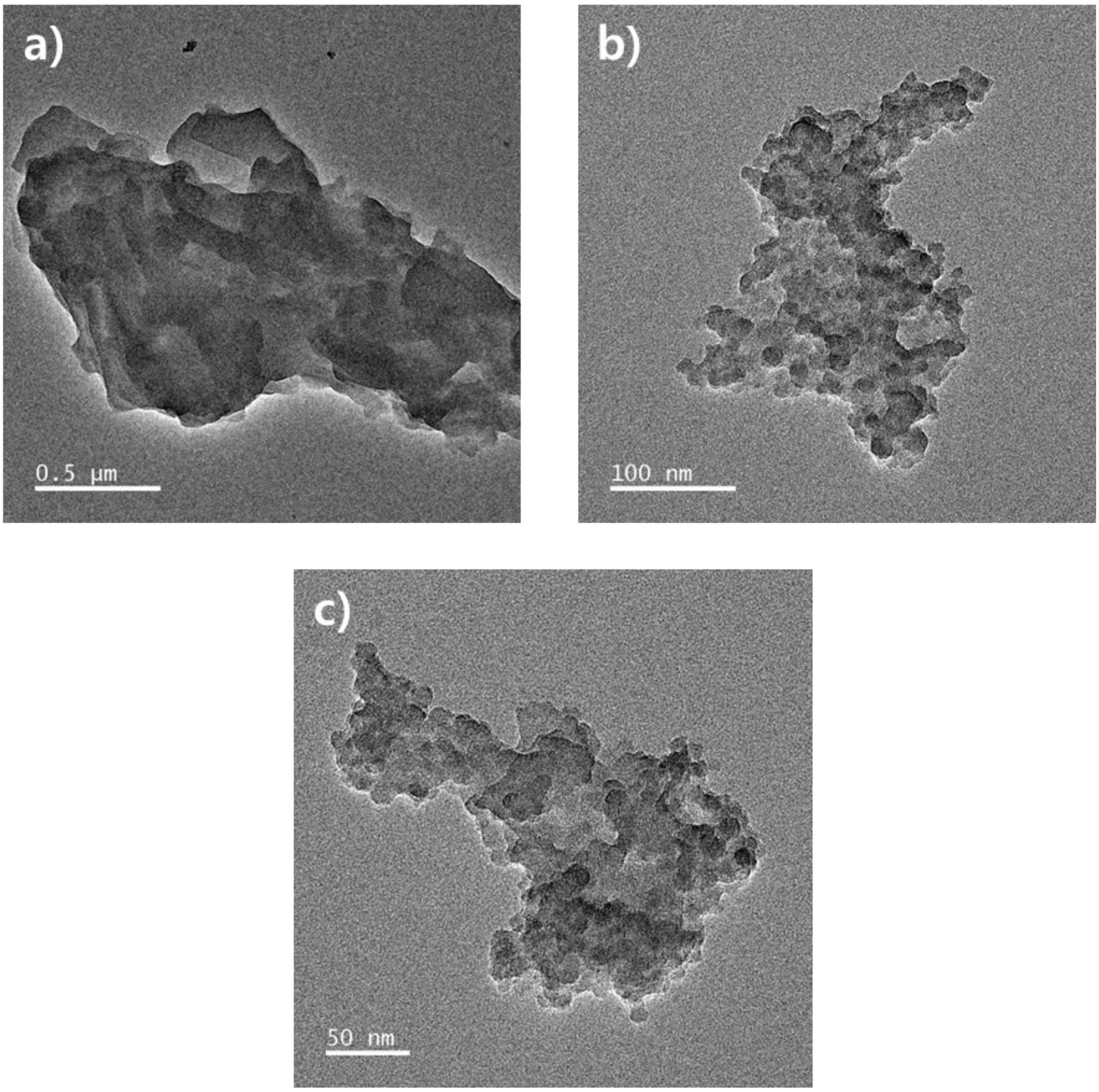

Figure S10. TEM images of TPC2-(Z) under various magnifications.

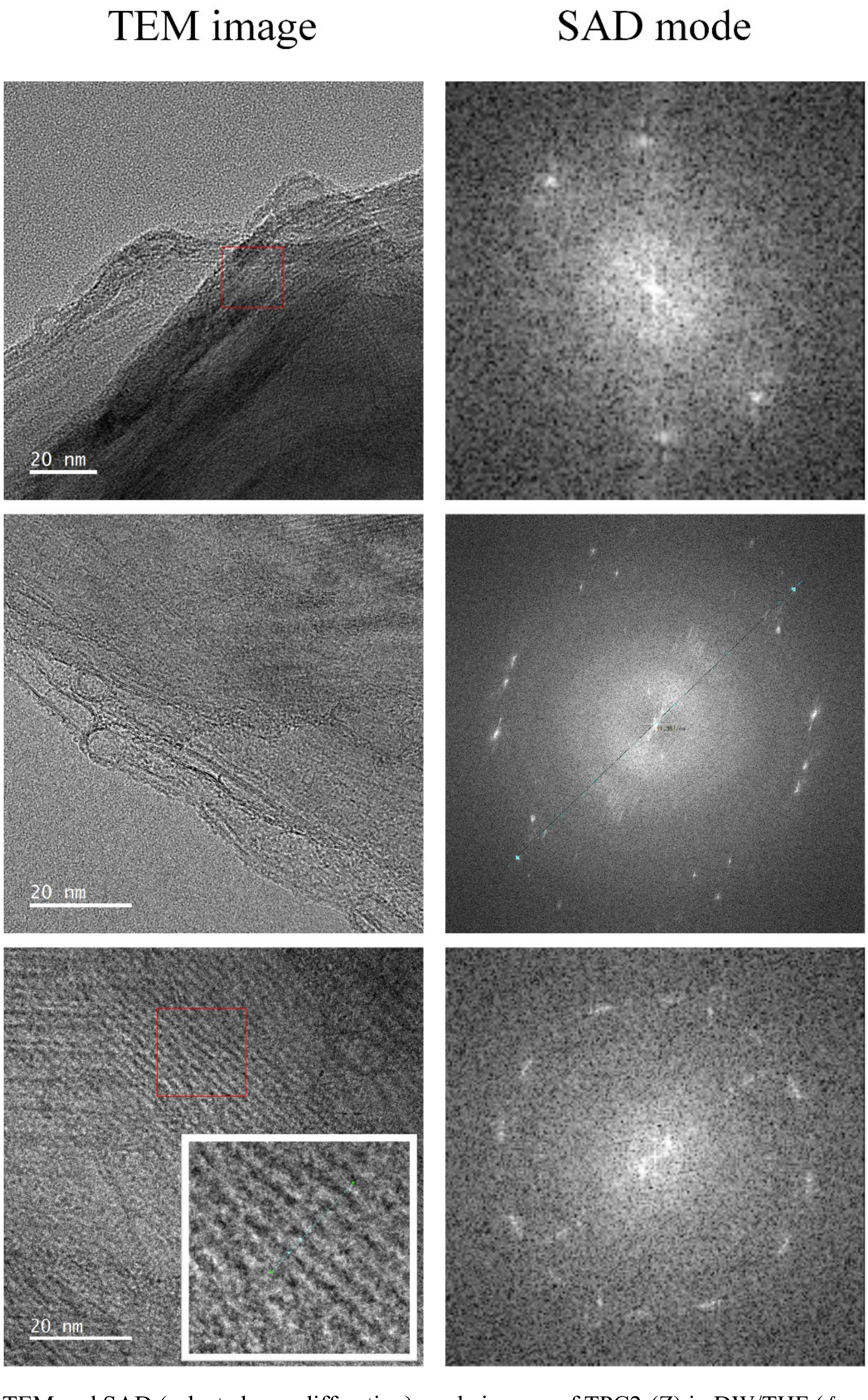

Figure S11. TEM and SAD (selected area diffraction) mode images of TPC2-(Z) in DW/THF (f_w = 90 %). Magnified regions are encircled red. The inset in the lower most is the magnification of red encircled region.

[1.raw] 10 — **Peak Search Report**

SCAN: 5.0/90.0/0.02/0.4(sec), Cu(40kV,40mA), I(p)=6537, 05/25/23 12:43p

PEAK: 31(pts)/Parabolic Filter, Threshold=3.0, Cutoff=0.1%, BG=3/1.0, Peak-Top=Summit

NOTE: Intensity = Counts, 2T(0)=0.0(deg), Wavelength to Compute d-Spacing = 1.54059Å (Cu/K-alpha1)

#	2-Theta	d(Å)	Height	H%	Area	A%	FWHM	XS(Å)
1	6.500	13.5879	1507	27.8	15828	8.5	0.179	727
2	7.142	12.3672	306	5.7	4744	2.5	0.263	391
3	7.981	11.0692	475	8.8	3913	2.1	0.140	>1000
4	8.779	10.0640	448	8.3	5075	2.7	0.192	636
5	9.580	9.2247	1662	30.7	27916	14.9	0.285	351
6	11.902	7.4298	5232	96.7	73785	39.4	0.240	449
7	12.499	7.0761	912	16.9	25039	13.4	0.467	191
8	13.541	6.5341	1634	30.2	38918	20.8	0.405	226
9	14.541	6.0866	854	15.8	30858	16.5	0.614	141
10	16.759	5.2857	2437	45.0	50369	26.9	0.351	270
11	17.479	5.0696	3111	57.5	80606	43.1	0.440	206
12	18.161	4.8809	2592	47.9	112901	60.3	0.740	115
13	19.220	4.6142	5355	98.9	181661	97.1	0.577	152
14	20.060	4.4229	2108	38.9	48958	26.2	0.395	235
15	21.100	4.2070	5412	100.0	187100	100.0	0.588	149
16	21.919	4.0516	2606	48.2	72942	39.0	0.476	190
17	22.719	3.9108	1828	33.8	53095	28.4	0.494	182
18	23.400	3.7986	1358	25.1	50310	26.9	0.630	139
19	24.082	3.6925	827	15.3	27718	14.8	0.570	155
20	24.779	3.5902	505	9.3	14499	7.7	0.488	185
21	25.361	3.5090	689	12.7	12283	6.6	0.303	331
22	26.105	3.4107	265	4.9	4047	2.2	0.259	409
23	27.159	3.2807	216	4.0	2718	1.5	0.214	545
24	27.958	3.1887	539	10.0	15829	8.5	0.500	181
25	28.459	3.1338	313	5.8	9460	5.1	0.513	176
26	29.924	2.9836	196	3.6	3372	1.8	0.292	351
27	30.853	2.8958	110	2.0	799	0.4	0.124	>1000
28	31.735	2.8173	176	3.3	2669	1.4	0.258	418
29	34.324	2.6105	113	2.1	1173	0.6	0.176	781
30	34.503	2.5974	150	2.8	1278	0.7	0.145	>1000
31	34.981	2.5630	139	2.6	771	0.4	0.094	>1000
32	36.280	2.4741	84	1.5	463	0.2	0.094	>1000
33	41.474	2.1755	83	1.5	442	0.2	0.090	>1000
34	42.391	2.1305	115	2.1	1400	0.7	0.207	601
35	47.239	1.9226	67	1.2	916	0.5	0.232	512
36	47.523	1.9117	90	1.7	1724	0.9	0.326	321
37	48.345	1.8811	51	0.9	332	0.2	0.111	>1000
38	54.017	1.6962	63	1.2	507	0.3	0.138	>1000
39	59.819	1.5448	63	1.2	309	0.2	0.083	>1000
40	62.060	1.4943	53	1.0	501	0.3	0.160	>1000
41	76.763	1.2406	61	1.1	301	0.2	0.084	>1000
42	83.896	1.1524	44	0.8	459	0.2	0.176	>1000

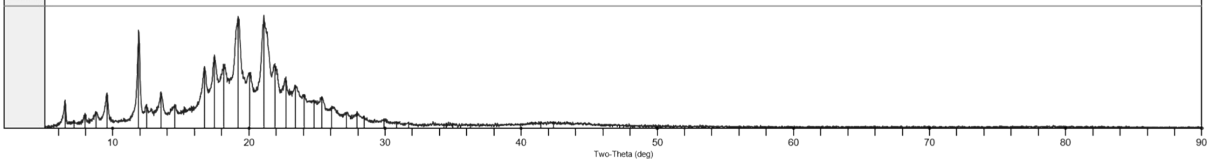

Figure S12. Powder XRD result of TPC2-(Z) peak analysis.

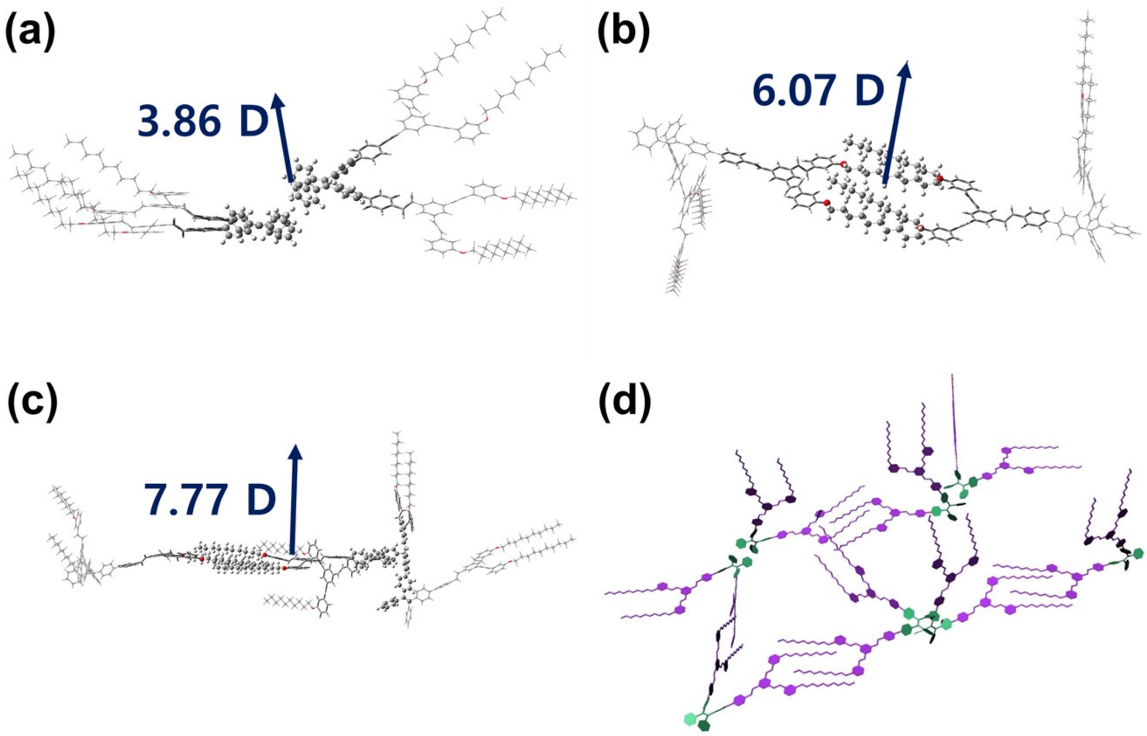

Figure S13. Energy minimized optimized structures of TPC2-(Z) and dipole moments having a) TPE-TPE interaction, b) clip-clip (DOS) interaction, c) both interactions and d) a combined structure on the interaction between molecules via TPE aggregation (olive) and DOS unit clipping (purple), based on DFT calculations.

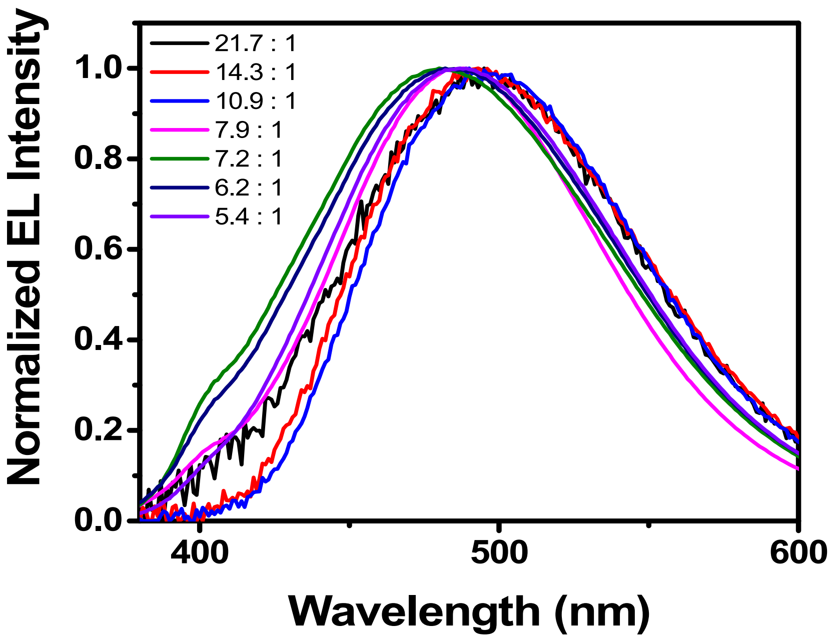

Figure S14. Electroluminescence spectra of TPC2-(Z) at different (host : guest) molar ratio compositions at maximum luminescence under a VCL driving measurement. Detailed LEC performances are listed in Table S3.

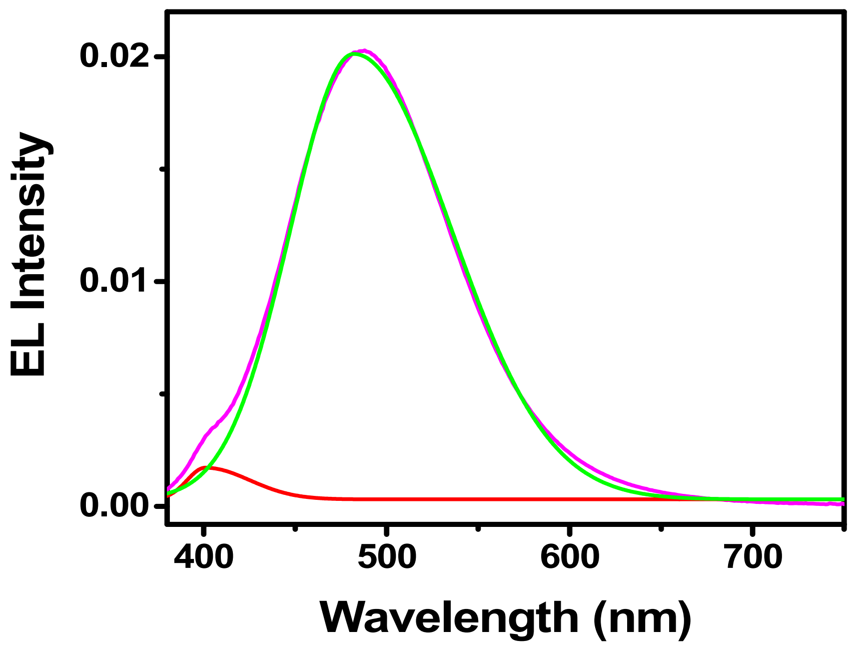

Figure S15. Peak deconvolution of EL spectra Figure 3b, 11.1V (magenta – original peak, green and red – deconvoluted).

S-4. Ferroelectric and piezoelectric characterization of TPC2-(Z)

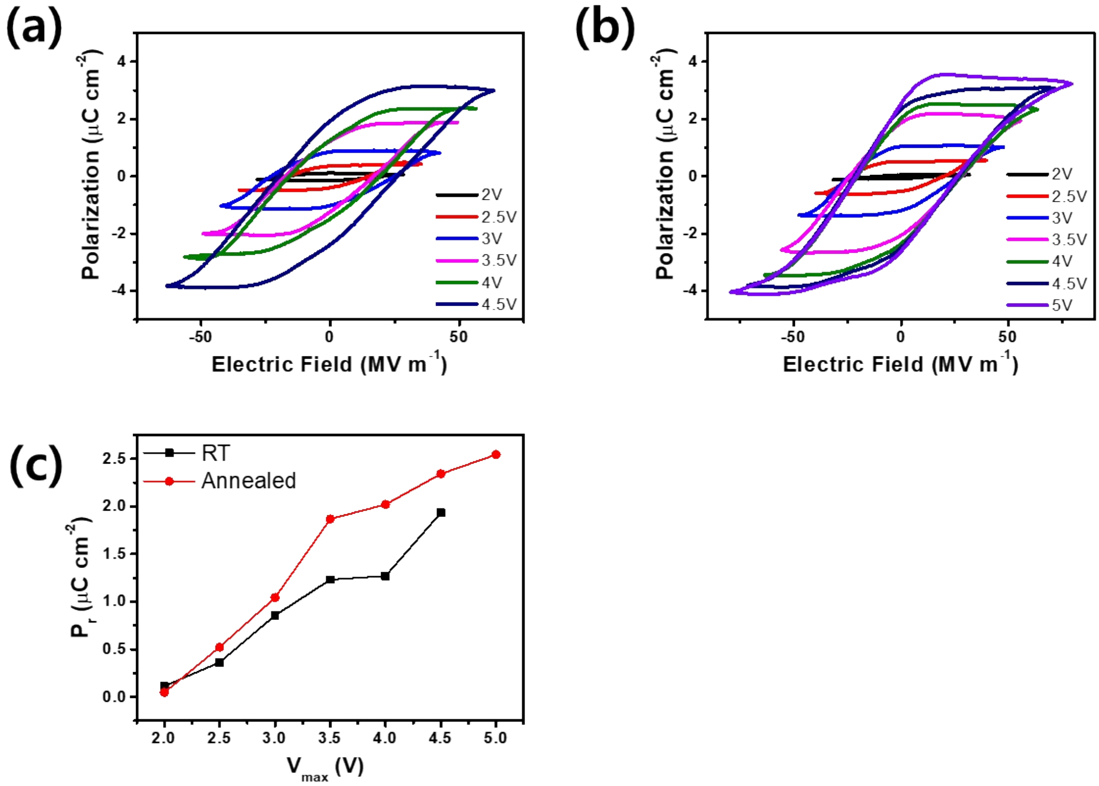

Figure S16. a) Polarization – electric field loops of TPC2-(Z) thin film and b) result of annealed film. c) Remnant polarization (P_r) with varying V_{max} value.

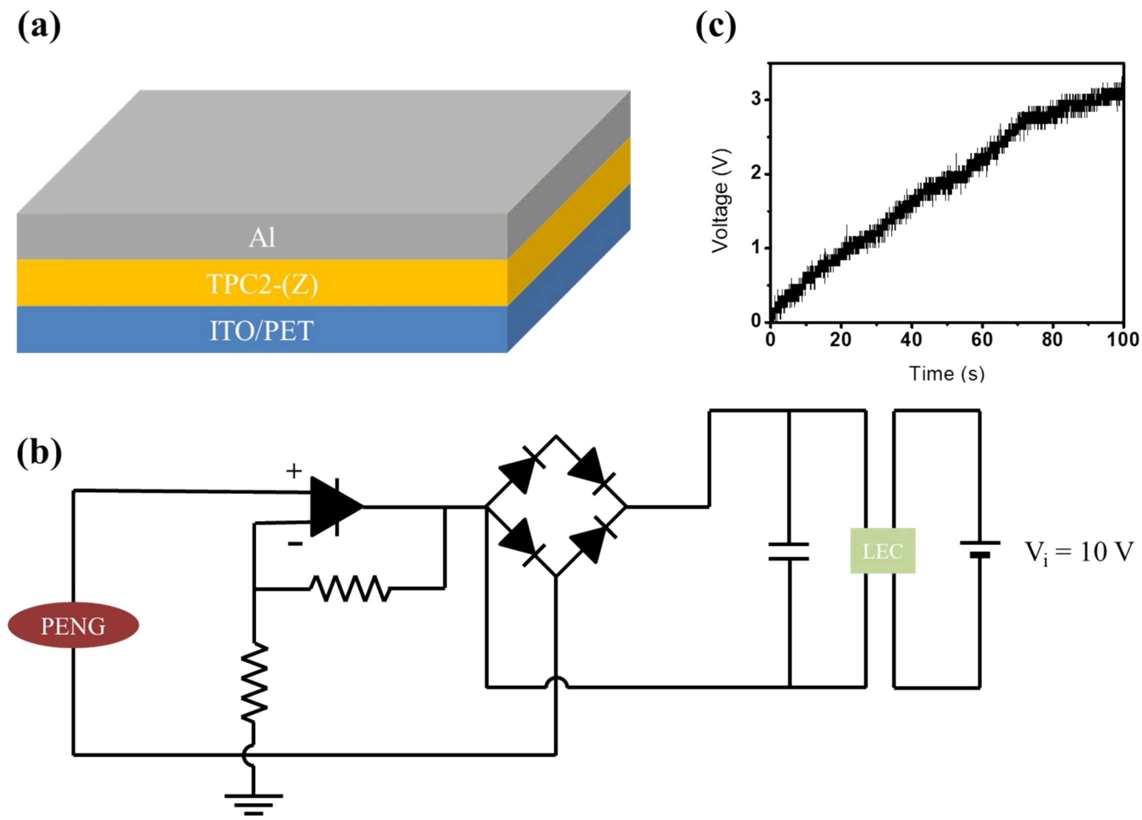

Figure S17. a) Structure of PENG. b) The circuit diagram of piezoelectrically operated EL device, and c) the curve of the storage voltage by physical bending of PENG at a frequency of 1 Hz.

Determination of longitudinal piezoelectric coefficient (d^*_{33})

Longitudinal piezoelectric coefficient (d^*_{33}). was obtained from equation S1 and S2,[1]

Equation (S1):

$$\text{Piezoelectric Amplitude [m]} = \frac{3 \cdot \text{PFM Amplitude [V]}}{\text{Sensitivity [V/m]} \cdot \text{Gain Correction Factor}}$$

Equation (S2):

$$d^*_{33}\ \text{[m/V]} = \frac{\text{Piezoelectric Amplitude [m]}}{\text{Tip Bias [V]}}$$

where PFM amplitude is measured in voltages (V) from the lock-in amplifier. Sensitivity (V/m), the calibration factor that converts voltage signals to displacement was determined from the PFM amplitude data. Gain correction factor, an instrument-dependent amplification factor, which is related to signal to noise ratio during PFM experiments. Tip bias (V) is the AC voltage applied during PFM measurements. Using these values, the PFM amplitude data in mV unit was converted into pm unit (figure 4c), which showed four linear regions. The slopes for the linear region corresponds to the longitudinal piezoelectric coefficient as reported before.[2, 3, 4] From the PFM amplitude data in the figure 4c, we obtained four distinct slopes in the linear regions, which were averaged to yield d_{33} = -23.8 pm V^{-1}.

Table S1. d-spacing distances of TPC2-(Z) by various experimental methods.

XRD			Assignment	DFT	DFT (optimized)		
2θ [°]	d [nm]	Intensity [counts]		d [nm]	d [nm]	Interaction [a)]	
6.50	13.59	1507	d_1	13.80	13.84	Clip-Clip	C(πB)-C(decyl)
7.98	11.07	475	d_2	11.58	11.55, 11.02	Length of Clip unit, TPE-TPE	C(decyl)-C(decyl), C(πB)-C(πT)
9.58	9.22	1662	d_3	9.58	10.28	TPE-TPE	ethene-ethene
11.90	7.43	5232	d_4	7.29	7.82	TPE-TPE	C(πB)-C(πT)
12.50	7.08	912	d_5	7.07	6.39	Clip-Clip	Self-assembly (C-C)
13.54	6.53	1634	d_6	6.65	6.55	Clip-Clip	Self-assembly (C-C)
16.76	5.29	2437	d_7	5.38	-	TPE-TPE	C(πB)-C(πT)
				5.31	5.41	Clip-Clip	Self-assembly (C-C)
17.48	5.07	3111	d_8	5.06	5.02	TPE-TPE	C(πB)-C(πT)
19.22	4.61	5355	d_9	4.40	4.81	TPE-TPE	C(πB)-C(πT)
20.06	4.42	2108	d_9	4.14	4.27	TPE-TPE	C(πB)-C(πT)
			d_9	4.26	4.37	TPE-TPE	C(πT)-C(πT)
21.92	4.05	2606	d_{10}	4.05	4.08	TPE-TPE	C(πB)-C(πT)
22.72	3.91	1828	d_{11}	3.85	3.89	TPE-TPE	C(πB)-C(πT)
23.40	3.80	1358	d_{12}	3.89	-	TPE-TPE	C(πT)-C(πT)
25.36	3.51	689	d_{13}	3.66	-	TPE-TPE	C(πB)-C(πT)
27.16	3.28	216	d_{14}	3.39	3.65	TPE-TPE	C(πT)-H(T)
29.92	2.98	196	d_{14}	3.06	3.37	TPE-TPE	C(πT)-H(T)
30.85	2.90	110	d_{14}	3.00	3.04	TPE-TPE	C(πB)-H(T)
31.74	2.82	176	d_{14}	2.85	2.94	TPE-TPE	C(πB)-H(T)
			d_{20}	19.31	18.53	Clip-Clip	C(πB)-C(πB)
			d_{21}	64.71	64.18	TPE-TPE	C(πT)-C(πT)
			d_{22}	58.14	57.00	TPE-TPE	C(πT)-C(πT)
			d_{23}	12.62	12.98	TPE-TPE	C(πT)-C(πT)

d_{24}	14.77	13.44	TPE-TPE	C(πT)-C(πT)
d_{25}	21.59	23.19	TPE-TPE	C(πB)-C(πB)

Table S2. Comparison of organic ferroelectric materials.

Organic ferroelectric material	**P_r [μC cm^{-2}]**	**d^*_{33} [pm V^{-1}]**	**d_{33} [pC N^{-1}]**
TPC2-(Z)	2.54	-23.8	
TPC1[1]	1.93	-9.3	-8.1±1.9
TPC4[1]	2.27	-17.4	-15.5±2.4
BTA[2]	6	20	
4,5-dibromo-2-methyl-1H-imidazole[5]	-	2.6	
croconic acid[6, 7]	~30	7.6	
3-hydroxy-1*H*-phenalen-1-one[6, 7]	5.6	3.1	
Phenylmalonaldehyde[6, 7]	9	4.3	

Piezoelectric amplitude [m] = 3 · PFM amplitude [V] / sensitivity [V/m] / gain correction factor

Piezoelectric coefficient (d^*_{33}) [m/V] = piezoelectric amplitude [m] / tip bias [V]

Table S3. Compositions of LEC fabrication trials**.**

Trial[a)]	CBP (µmol)	TPC2-(Z) (µmol)	Molar ratio[b)]
1	18.00	0.83	21.7 : 1
2	16.78	1.17	14.3 : 1
3	15.77	1.45	10.9 : 1
4	14.45	1.82	7.9 : 1
5	14.01	1.95	7.2 : 1
6	13.29	2.15	6.2 : 1
7	12.63	2.34	5.4 : 1

a) The amount of $THABF_4$ electrolyte is fixed to 2.36 mg

b) Total weight of CBP and TPC2Z is maintained to 10.14 mg

Table S4. List of TPC2-(Z) LEC performances in VCL mode.

(Host : Guest) molar ratio	V_{on} [V]	Lv_{max} [$Cd \cdot m^{-2}$]	V_{max} [V]	CE [$cd \cdot A^{-1}$]	J [$mA \cdot cm^{-1}$]	λ_{EL} [nm]	Reference
11.9 : 1 (TPC2-(E/Z))	7.5	445.4	10.4	0.23	205.7	483	1
21.7 : 1	14.1	7.6	14.8	0.0045	169.0	495	-
14.3 : 1	14.1	15.5	15.2	0.012	126.5	493	-
10.9 : 1	14.6	21.2	17.1	0.030	70.1	491	-
7.9 : 1	9.9	627.1	11.2	0.33	192.4	487	-
7.2 : 1	11.9	709.1	12.2	0.26	269.9	480	-
6.2 : 1	11.7	526.3	12.2	0.35	148.8	482	-
5.4 : 1	11.9	723.8	12.2	0.34	211.4	487	-

Table S5. List of TPC2-(Z) LEC performances in PCL mode.

(Host : Guest) molar ratio	V_{on} [V]	Lv_{max} [$cd \cdot m^{-2}$]	V_{max} [V]	CE [$cd \cdot A^{-1}$]	J [$mA \cdot cm^{-1}$]	λ_{EL} [nm]	Reference
11.9 : 1 (TPC2-(E/Z))	4.3	685.8	7.3	-	1.9	483	1
21.7 : 1	6.3	14.3	9.3	-	20.0	489	-
14.3 : 1	8.7	22.0	9.9	-	72.2	491	-
10.9 : 1	8.5	75.9	9.3	-	24.4	492	-
7.9 : 1	3.9	890.7	7.4	-	120	486	-
7.2 : 1	6.2	337.9	10.1	-	236.7	480	-
6.2 : 1	7.4	1007.0	9.1	-	248.9	486	-
5.4 : 1	6.3	458.5	6.3	-	140	481	-

Reference

1. D. Kim, H. T. T. Thuy, B. Kim, Y. Auh, M. Rémond, K. K. Leong, T. Liang, J. Kim and E. Kim, *Advanced Functional Materials*, 2023, **33**, 2208157.
2. I. Urbanaviciute, X. Meng, M. Biler, Y. Wei, T. D. Cornelissen, S. Bhattacharjee, M. Linares and M. Kemerink, *Materials Horizons*, 2019, **6**, 1688-1698.
3. R. Haldar, A. Kumar, D. Mandal and M. Shanmugam, *Materials Horizons*, 2024, **11**, 454-459.
4. A. Jalalian, A. M. Grishin, X. L. Wang, Z. X. Cheng and S. X. Dou, *Applied Physics Letters*, 2014, **104**.
5. M. Owczarek, K. A. Hujsak, D. P. Ferris, A. Prokofjevs, I. Majerz, P. Szklarz, H. Zhang, A. A. Sarjeant, C. L. Stern, R. Jakubas, S. Hong, V. P. Dravid and J. F. Stoddart, *Nature Communications*, 2016, **7**, 13108.
6. S. Horiuchi, J. y. Tsutsumi, K. Kobayashi, R. Kumai and S. Ishibashi, *Journal of Materials Chemistry C*, 2018, **6**, 4714-4719.
7. S. Horiuchi, K. Kobayashi, R. Kumai and S. Ishibashi, *Nature Communications*, 2017, **8**, 14426.